⌘ *Author's Choice*

THE JOURNAL OF BIOLOGICAL CHEMISTRY VOL. 287, NO. 14, pp. 11011–11017, March 30, 2012

Uroplakins Do Not Restrict CO_2 Transport through Urothelium*

Received for publication, January 3, 2012, and in revised form, February 2, 2012 Published, JBC Papers in Press, February 7, 2012, DOI 10.1074/jbc.M112.339283

Florian Zocher[‡], Mark L. Zeidel[§], Andreas Missner[‡], Tung-Tien Sun[¶], Ge Zhou[¶], Yi Liao[¶], Maximilian von Bodungen[§], Warren G. Hill[§], Susan Meyers[‖], Peter Pohl[‡1], and John C. Mathai[§]

From the [‡]Institut für Biophysik, Johannes Kepler Universität, 4020 Linz, Austria, the [§]Department of Medicine, Beth Israel Deaconess Medical Center, Boston, Massachusetts 02215, the [¶]Departent of Cell Biology, New York University, New York, New York 10016, and the [‖]Department of Medicine, University of Pittsburgh, Pittsburgh, Pennsylvania 15260

Background: The tightness of various membrane barriers to CO_2 is of unknown molecular origin.
Results: The bladder tissue lacks carbonic anhydrase. The resulting low intra-epithelial CO_2 concentration gives rise to the apparent CO_2 impermeability.
Conclusion: Uroplakins do not act to decrease transepithelial CO_2 flux.
Significance: Enzymatic regulation of CO_2 abundance rules out that aquaporins significantly contribute to the maintenance of acid base homeostasis.

Lipid bilayers and biological membranes are freely permeable to CO_2, and yet partial CO_2 pressure in the urine is 3–4-fold higher than in blood. We hypothesized that the responsible permeability barrier to CO_2 resides in the umbrella cell apical membrane of the bladder with its dense array of uroplakin complexes. We found that disrupting the uroplakin layer of the urothelium resulted in water and urea permeabilities (P) that were 7- to 8-fold higher than in wild type mice with intact urothelium. However, these interventions had no impact on bladder P_{CO2} ($\sim 1.6 \times 10^{-4}$ cm/s). To test whether the observed permeability barrier to CO_2 was due to an unstirred layer effect or due to kinetics of CO_2 hydration, we first measured the carbonic anhydrase (CA) activity of the bladder epithelium. Finding none, we reduced the experimental system to an epithelial monolayer, Madin-Darby canine kidney cells. With CA present inside and outside the cells, we showed that P_{CO2} was unstirred layer limited ($\sim 7 \times 10^{-3}$ cm/s). However, in the total absence of CA activity P_{CO2} decreased 14-fold ($\sim 5.1 \times 10^{-4}$ cm/s), indicating that now CO_2 transport is limited by the kinetics of CO_2 hydration. Expression of aquaporin-1 did not alter P_{CO2} (and thus the limiting transport step), which confirmed the conclusion that in the urinary bladder, low P_{CO2} is due to the lack of CA. The observed dependence of P_{CO2} on CA activity suggests that the tightness of biological membranes to CO_2 may uniquely be regulated via CA expression.

The urinary bladder, which stores urine of a composition vastly different from that of blood, exhibits extremely low permeability to water and solutes such as urea and other metabolites in the urine (1, 2). The urine osmolality varies widely between 50 and 1000 mosmol/kg compared with near constant osmolality of blood of ~ 290 mosmol/kg. The primary permeability barrier of the bladder is formed by the umbrella cells whose apical side faces the lumen along with the tight junctions (2–4). The apical surface of these cells contains urothelial plaques, which cover ~90% of the membrane surface of the bladder. These plaques are made of a paracrystalline array of proteins consisting of a family of integral membrane proteins known as uroplakins (UPs), which include UPIa, UPIb, UPII, UPIIIa and UPIIIb proteins (5, 6). The urinary bladders of UPIIIa-deficient mice showed a marked diminution of plaque surface area and significantly enhanced water and urea permeability, which suggested that uroplakins represent a significant component of the apical membrane barrier to water and solute flux across the bladder (3, 5–7).

When the kidney excretes acidic urine, P_{CO2} of urine reaches 80–100 mm Hg, 3–4-fold higher than the blood P_{CO2} (8–10). The accumulation of CO_2 in the bladder and its failure to diffuse down its concentration gradient suggest that the permeability of the bladder to CO_2 might be very low. We have shown previously that gases such as CO_2 and H_2S are freely permeable across the lipid membrane and are limited only by the unstirred layer adjacent to the membrane (11, 12). Because the umbrella cell apical membrane forms a barrier to water and solute flux (1, 3, 13), we hypothesized that this specialized membrane may also act as a barrier to CO_2 flux.

We measured the CO_2 flux across a normal urothelium and urothelium in which apical barrier function was disrupted. We found that disrupting apical membrane barrier function by protamine sulfate treatment or by genetic ablation of uroplakins (II/IIIA) resulted in water and urea permeabilities that were 7- to 8-fold higher than in wild type mice with intact urothelium. However, these interventions had no impact on CO_2 permeability across the bladder. To test whether the observed permeability was due to an unstirred layer effect or due to kinetics of CO_2 hydration, we measured the CO_2 perme-

* The project was supported by Grant Numbers DK048217 (to M. L. Z.) and R01DK083299 (to W. G. H.) from the National Institute of Diabetes and Digestive and Kidney Diseases. This work was also supported by Austrian Science Fund (FWF) Grant P23466 (to P. P.).
⌘ *Author's Choice*—Final version full access.
[1] To whom correspondence should be addressed: Johannes Kepler Universität Linz, Gruberstrasse 40, 4020 Linz, Austria. Tel.: 0043-732-2428-7562; Fax: 0043-732-2428-7563; E-mail: peter.pohl@jku.at.

ability in Madin-Darby canine kidney (MDCK)[2] cells in the presence and absence of carbonic anhydrase inhibitor. Our studies show that the lowered permeability of CO_2 across the bladder is mainly due to a lack of carbonic anhydrase (CA) in the urothelium.

EXPERIMENTAL PROCEDURES

Generation of Uroplakin II/III Knock-out Mice—The generation and characterization of the UPIIIa and UPII knock-out mice were described previously (23, 24). UPII/UPIIIa double knock-out mice were generated by cross-breeding UPII and UPIIIa knock-out mice. To identify the UPII/IIIa homozygote, the following primer pairs were used for genotyping. For deletion of UPII gene, one forward (5′-TCCCACTCCGAGACAAAATC-3′) and two reverse (5′-TATCGCCTTCTTGACGAGTTC-3′ for detecting a 600-bp product of the neomycin sequence were used, and 5′-TCCCACCAGCAATAGAGACC-3′ was used for a 198-bp product of the native UPII gene. For deletion of the UPIIIa gene, forward (5′-GGACCGGACTGTATGCAAAT-3′) and reverse (5′-TATCGCCTTCTTGACGAGTTC-3′) primers were used; for detecting a 700-bp product of the neomycin sequence, forward (5-CACCTCCTCTTTTGCTTTGA-3) and reverse (5-GCCCACTTACATCCCAGTTT-3) for a 250-bp product of the native UPIIIa gene were used.

Measurement of Urothelial Barrier Function—Animal experiments were performed in accordance with the animal use and care committees of New York University, University of Pittsburgh, Beth Israel Deaconess Medical Center, and Johannes Kepler University. Bladders were excised after lethal anesthesia, washed in placed in NaCl-Ringer buffer (110 mM NaCl, 5.8 mM KCl, 25 mM $NaHCO_3$, 1.2 mM KH_2PO_4, 2.0 mM $CaCl_2$, 1.2 mM $MgSO_4$, and 11.1 mM glucose (pH 7.4) at 37 °C, bubbled with 95% O_2, 5% CO_2 gas) and carefully stretched and mounted on a small ring in the same solution at 37 °C. The bladder was then placed in a modified Ussing chamber (11). Both compartments of the chamber were under constant stirring and temperature control and allowed electrical measurements and sampling.

In all other transepithelial resistance measurements both voltage-sensing and current-passing electrodes were connected to an automatic voltage clamp (EC-825, Warner Instruments, Hamden, CT), which was, in turn, connected to a microcomputer with a MacLab interface (3, 11). All permeability measurements were performed at 37 °C after stabilization of the transepithelial resistance. Diffusive water and urea permeability coefficients were determined by using isotopic fluxes as described (13, 27). Briefly, tritiated water (1 μCi/ml) or [^{14}C]urea (0.25 μCi/ml) were added to the apical chamber and 100-μl samples of both apical and basolateral chambers were taken every 15 min. Sample volumes were replaced quantitatively with warmed NaCl-Ringer. Sample radioactivities were counted with a liquid scintillation counter (model 1500, Packard Tri-Carb), and flux rates and permeabilities were calculated as described previously (13, 27).

Carbonic Anhydrase Activity Measurement—Carbonic anhydrase activity of bladder tissue was measured by pH electrometric method (28). Briefly, we added 2 ml of CO_2 saturated water to 3 ml of a Tris-sulfate solution (pH 8.3) and monitored the time that elapsed until pH dropped to 6.3. CA activity of bladder tissue was measured similarly by adding bladder tissue homogenate (100 μg of protein). The bladder musculature was dissected away before homogenization. All CA activities were measured on ice.

Protamine Sulfate Treatment and Confocal Imaging—Protamine sulfate was instilled into mouse bladder transuretherally using a lubricated catheter under light halothane anesthesia. Protamine sulfate (PS) was instilled was instilled as a bolus (100 μl of 15 mg/ml PS in PBS) for 15 min before emptying, and the animals were euthanized. Mouse bladders were removed according to animal protocols, and its muscle layers were dissected away. These bladders were mounted in modified Ussing chamber and washed in PBS, and its permeability to water and urea were measured as described above. For CO_2 studies, the bladders were mounted in the Ussing chambers, and protamine sulfate (15 mg/ml) was then added to the apical or luminal surface and incubated for 15 min. The tissue was washed with PBS at the end of incubation and fixed for antibody staining and confocal imaging as described previously (29). Monoclonal antibody for uroplakin II was a kind gift from Dr. Apodaca, University of Pittsburgh. F-actin and nuclei was visualized by using Alexa Fluor® 546 phalloidin and Topro-3 probes respectively. Both these probes and secondary antibodies were purchased from Invitrogen.

Cell Culture—Stably aquaporin-1-overexpressing Madin-Darby canine kidney (MDCK-AQP1) cells (30), and MDCK cells were cultured in DMEM supplemented with 110 mg/liter sodium pyruvate, 584 mg/liter L-glutamine, non-essential amino acids, 5% FCS, 20 mM HEPES, 0.1% $NaHCO_3$, and penicillin/streptomycin at 37° in 8.5% CO_2. For MDCK-AQP1, 75 μg/ml hygromycin B was added. For microelectrode measurements, the cells were seeded 1:1 onto semipermeable supports (Transwell, Costar) with a surface area of 0.33 cm^2 and cultured again until the electrical resistance reached >3 Kilo ohm, indicating a tight monolayer (usually after 3–4 days). All cell experiments were carried out in HBBS buffer at 37°.

CO_2 Flux Measurements—The flux of the weak acid CO_2 from the apical to the basolateral compartment of the Ussing chamber caused acidification of the external unstirred layers (USL) adjacent to the basolateral membrane as shown previously (11). The pH shift is a result of the following chemical reactions,

$$H^+ + OH^- \rightleftarrows H_2O$$

$$H^+ + HEPES \rightleftarrows HEPESH$$

$$CO_2 + H_2O \rightleftarrows H_2CO_3 \rightleftarrows H^+ + HCO_3^- \rightleftarrows H^+ + CO_3^{2-}$$

$$CO_2 + OH^- \rightleftarrows HCO_3^-$$

REACTIONS 1–4

Because both the CO_2 flux J_{CO2}^{USL} and the HCO_3^- flux J_{CO2}^{USL} through the USL contribute to the membrane CO_2 flux J_{CO2},

[2] The abbreviations used are: MDCK, Madin-Darby canine kidney; CA, carbonic anhydrase; PS, protamine sulfate; USL, unstirred layers; AQP1, aquaporin-1.

$$J_{CO_2} = J^{USL}_{HCO_3} + J^{USL}_{CO_2} \quad \text{(Eq. 1)}$$

the simplified diffusion model (15) is valid,

$$\frac{1}{J_{CO_2}} = \frac{1}{P^{USL}_{A^-}[HCO_3^-]} + \frac{1}{P_{CO_2}[CO_2]} \quad \text{(Eq. 2)}$$

where the bicarbonate concentration in the apical compartment $[HCO_3^-]$ is much larger than the bicarbonate concentration in the basolateral compartment. In the presence of CA, we assume the hydration and dehydration reactions of CO_2 to be in equilibrium because diffusion through the membrane or through adjacent unstirred layers is rate-limiting.

Equation 2 transforms the problem of determining P_{CO2} into the task of determining $J^{USL}_{HCO-3} = P^{USL}_{A-}[HCO_3^-]$. Because the only bicarbonate sink is the formation of CO_2, J^{USL}_{HCO3-} must be equal to the proton flux (J_P) through the USL. Due to the high buffer concentration the proton is carried by buffer molecules. The flux is calculated according to Ref. 31,

$$J^{USL}_{HCO_3^-} = J_P = D_B \frac{\beta \cdot \Delta pH}{\delta} \quad \text{(Eq. 3)}$$

where β, δ, and D_B are the buffering capacity of the solution, the USL thickness, and the buffer diffusion coefficient, respectively. We measured local pH as a function of the distance x to the epithelium. $\Delta pH/\delta$ was the first derivative of the experimental pH profiles at $x = 0$.

The proton-sensitive microelectrode had a tip size of 2–4 μm. Their 90% rise time was below 0.8 s. Addition of CA to the calibrating solution did not affect the sensitivity of the electrodes. Voltage recording was performed every second by an electrometer (model 6514; Keithley Instruments) connected via an IEEE-488 interface to a personal computer. A hydraulic microdrive manipulator (Narishige, Tokyo, Japan) moved the microelectrodes with a velocity of 2 μm s^{-1}.

We performed the experiments in HBBS buffer (118 mM NaCl, 4.6 mM KCl, 10 mM glucose, and 20 mM HEPES, pH 7.4) at 37 °C and applied the CO_2 gradient by adding $NaHCO_3$ and Na_2CO_3 to the apical side. Both sides of the measurement chamber contained CA (Sigma Aldrich). Magnetic stirrers continuously agitated the solutions.

RESULTS

First, we measured the flux of CO_2 across MDCK cell monolayers grown on filter supports and mounted in an Ussing type chamber (11). The CO_2 flux acidified the USL adjacent to the basal membrane. Increasing concentrations of bicarbonate in the apical medium led to increased acidification of the basolateral USL (Fig. 1, *top*). According to Equation 2, we plotted $1/J_{CO2}$ *versus* $1/[CO_2]$ and calculated the P_{CO2} to be 7×10^{-3} cm/s (Fig. 1, *top*, *inset*). Comparison of this value with the unstirred layer permeability, $P_{USL} = D_{CO2}/\delta = 2.9 \times 10^{-5}/1 \times 10^{-2}$ cm/s $= 2.9 \times 10^{-3}$ cm/s suggest that transport is limited by diffusion through the USL.

We measured P_{CO2} of the urinary bladder similarly by mounting the bladder on a circular holder with pins, which in turn separated the two halves of a modified Ussing type chamber. Both the apical and basal sides were bathed in modified

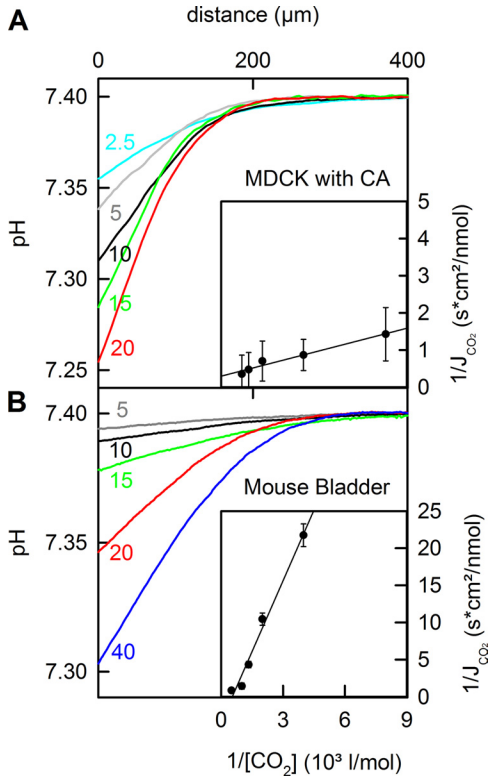

FIGURE 1. **CO_2 permeability of MDCK cells (*A*) and bladder (*B*): CO_2 flux-induced steady state pH shifts in the vicinity of MDCK cells was measured as a function of the distance to the cell monolayer or to the bladder at various apical HCO_3^- concentrations.** Increasing bicarbonate concentrations caused increasing acidification in the immediate monolayer/bladder vicinities. P_{CO2} of bladder and MDCK cells were determined from the linear regression shown in the insets (compare Equation 2) to be equal to 7×10^{-3} cm/s and 1.5×10^{-4} cm/s, respectively.

Ringer's solution. As shown in Fig. 1*B*, increased apical CO_2 concentrations caused increased USL acidification on the basal side of the bladder. Bladder P_{CO2} was equal to 1.5×10^{-4} cm/s (Fig. 1), which is ~45-fold lower than that of MDCK monolayers. These results confirmed that urothelium acts as a barrier to CO_2 transport.

We had shown previously that the urothelium has a very low permeability to water and urea and that the permeability barrier resides mainly in the uroplakin layer of the urothelium (4, 7). To investigate whether the uroplakins are also responsible for reduced permeability of CO_2, we selectively damaged the uroplakin layer by exposing the apical side of the bladder to PS. In rats, instillation of protamine sulfate (10 mg/ml) into bladders *in vivo* was shown to selectively damage the uppermost umbrella cell layer and caused enhanced leakage of urea and water from the bladder (4, 7). Fig. 2*A* shows that in mice, protamine sulfate treatment leads to a loss of umbrella cells and uroplakins. Staining and confocal imaging of bladder tissue sections using antibodies to uroplakin shows uroplakin II staining (Fig. 2, *green*) in control (Fig. 2*A*) and a loss of uroplakin II staining in protamine sulfate-treated bladder (Fig. 2*B*). The localization of cell layers in the bladder was visualized by staining for F-actin (*red*) and nuclei (*blue*). Fig. 2*B* clearly shows the loss of umbrella cells in the PS-treated bladder. Furthermore, the loss of umbrella cells disrupts apical membrane barrier function, as evidenced by a decrease in transepithelial resis-

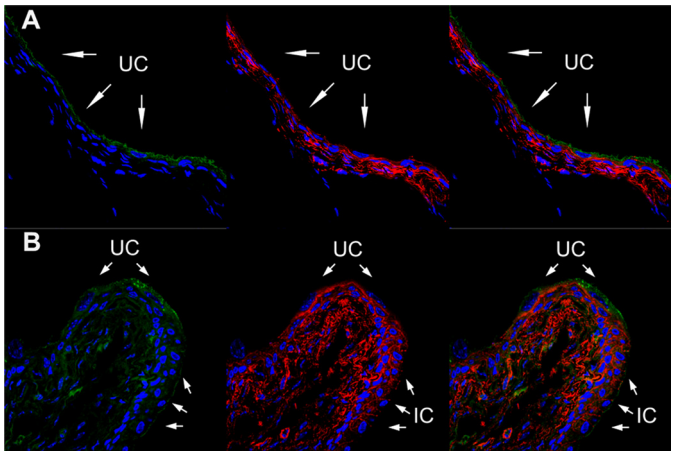

FIGURE 2. **Protamine sulfate treatment removes uroplakins and umbrella cells.** *A* (*upper panel*) shows control bladder showing uroplakin staining, green (*left*). Middle panel shows actin cytoskeleton and nuclear staining of the umbrella cells. Right most panel shows overlay of all three staining. *B* (*lower panel*), Protamine sulfate-treated cells show very little uroplakin staining (*left*) and loss of umbrella cells causing exposure of intermediate cells (*right*). *UC*, umbrella cell; *IC*, intermediate cell.

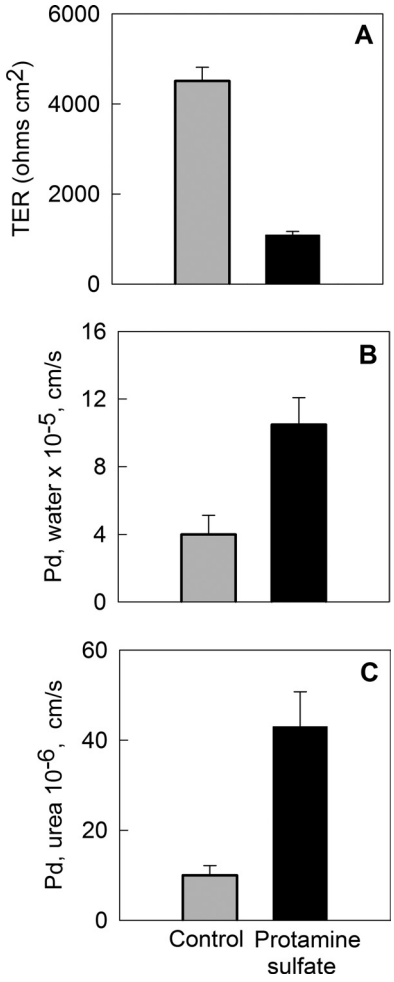

FIGURE 3. **PS treatment and bladder permeability.** PS exposure leads to decrease in transepithelial resistance (*TER*; *A*) and increased permeability to water, (*Pd, water*) (*B*) and to urea (*Pd, urea*) (*C*). Standard *error bars* are shown. Control (*n* of 6) and PS-treated mice (*n* of 10) are shown.

tance and ~3-fold increase in water and urea permeability (Fig. 3). PS treatment in rats was shown to selectively remove umbrella cells from the urothelium without causing inflammation (4, 7).

Although our confocal studies indicate that protamine sulfate treatment selectively damaged the upper urothelial layers, we used a second method to enhance the apical membrane leakiness by genetic ablation of uroplakins II and IIIa. The bladders from UPII knock-out mice were shown to be devoid of uroplakin plaques (14). Fig. 4 shows that in contrast to PS-treated bladders, in knock-out mice, $UPII^{-}/UPIIIa^{-}$ bladders lacking uroplakins the transepitheial resistance did not change. However, there was ~ 9-fold increase in water permeability and an ~8-fold increase in urea permeability, which shows that uroplakins indeed form a permeability barrier to these molecules.

To determine whether uroplakin removal increases P_{CO2}, we measured USL acidification in the presence of a CO_2 gradient. Fig. 5 shows that the pH profiles generated by CO_2 flux across wild type, uroplakin knock-out, and protamine sulfate-treated mice bladders are similar. These results show that ablation of uroplakins by protamine sulfate treatment and genetic knock-out does not increase the membrane leakiness to CO_2, although it does so for water and urea. Furthermore, these results also suggest that in contrast to the physical nature of the barrier for water and urea flux, the barrier to CO_2 transport may not be physical in nature. Rather, it may be (i) the thickness of the multiple urothelial cell layers causing diffusional limitations or (ii) low CA concentrations leading to slow down of the hydration-dehydration of CO_2. Because at physiological pH the equilibrium between bicarbonate and CO_2 is shifted to 95% in favor of the anionic form and as bicarbonate is membrane impermeable, this chemical reaction accompanies every CO_2 passage across a membrane. If not facilitated by CA, the reaction rate becomes the rate-limiting transport step, a scenario that recurs every time CO_2 crosses one of the multiple membrane barriers of the urothelium.

To identify the nature of the CO_2 permeability barrier, we studied the kinetics of CO_2 hydration and dehydration. It is known that hydration-dehydration reactions of CO_2 are very slow at neutral pH with a rate constant of 14 s^{-1} (for dehydration, K_{-2}) in absence of CA enzyme (15). To test whether the CO_2 hydration-dehydration reaction is the rate-limiting step for CO_2 permeation, we measured the CA activity of the bladder. A homogenate of bladder tissue devoid of musculature did not show any measurable CA activity and was similar to that of the control containing only the buffer (Fig. 6). As a positive control, we measured the CA activity of mouse blood and the activity of purified carbonic anhydrase at various enzyme concentrations. This result suggests that the lack of CA activity leads to the reduced CO_2 permeability of the urothelium.

To unambiguously show that absence of CA lowers the apparent CO_2 permeability, we recapitulated the bladder permeability results in MDCK monolayers. These cells have the advantage of an intrinsically active CA. Adding CA also to the bathing solution produced rather large pH shifts in the USL in response to a transepithelial CO_2 gradient (Fig. 7). P_{CO2} was equal to 7×10^{-3} cm/s, indicating that the system was USL-limited (Fig. 8). Omitting CA from the bathing solution

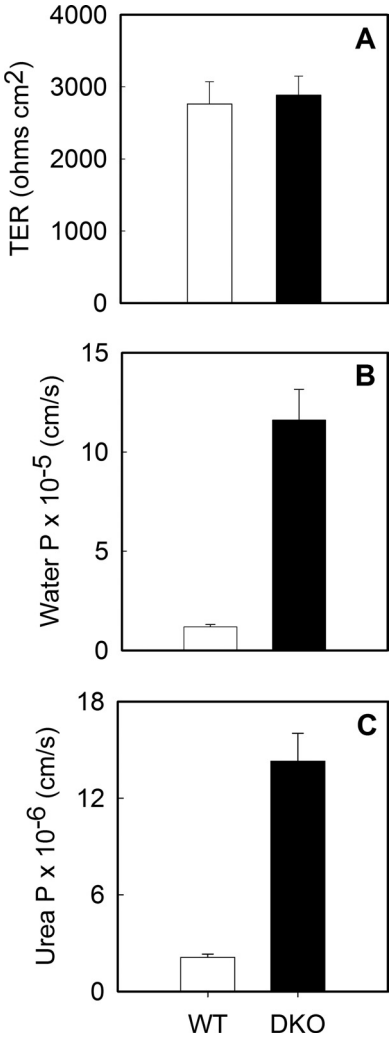

FIGURE 4. **Permeability of bladder of uroplakin knock-out mice lacking uroplakin plaques.** *A* shows that transepithelial resistance (*TER*) is normal, whereas water (*B*) and urea leakage (*C*) are significantly higher in mice bladder lacking uroplakins. Standard *error bars* are shown. Control (*n* of 5) and knock-out (*n* of 7) are shown.

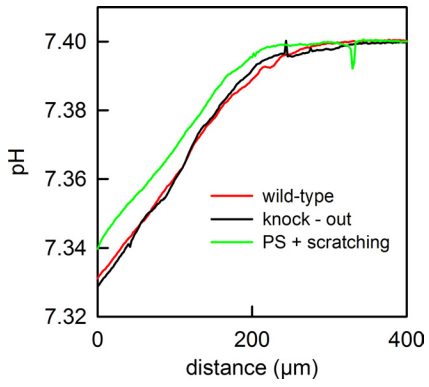

FIGURE 5. **Bladder P_{CO2} does not depend on the presence of the uroplakin layer.** CO_2 flux through the bladder monitored in terms of steady-state pH as a function of the distance to the membrane. Wild type mouse urinary bladder (*red*), the uroplakin knock-out bladder (*black*), and the urinary bladder treated with 10 mg/ml protamine sulfate and additional mechanical scratching (*green*) showed no difference in CO_2 permeability.

decreased the pH shift, which mimicked a drop in P_{CO2}. Inhibition of intracellular CA by acetazolamide further reduced the pH shift in the USL. The apparent P_{CO2} value of 5×10^{-4} cm/s

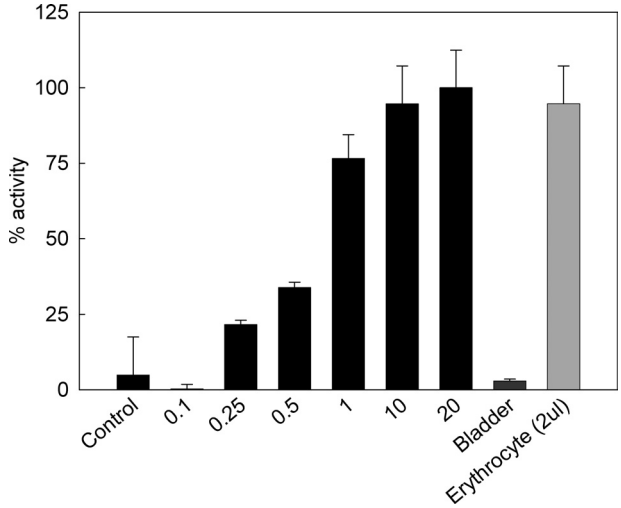

FIGURE 6. **CA activity of bladder.** Increasing amounts (units) of CA show increasing carbonic anhydrase activity (activity of 20 units of CA was normalized to 100% activity). Homogenized bladder tissue (muscle layer was dissected away) does not show any measurable CA activity. As an alternative control, 2 μl of mice blood shows high CA activity.

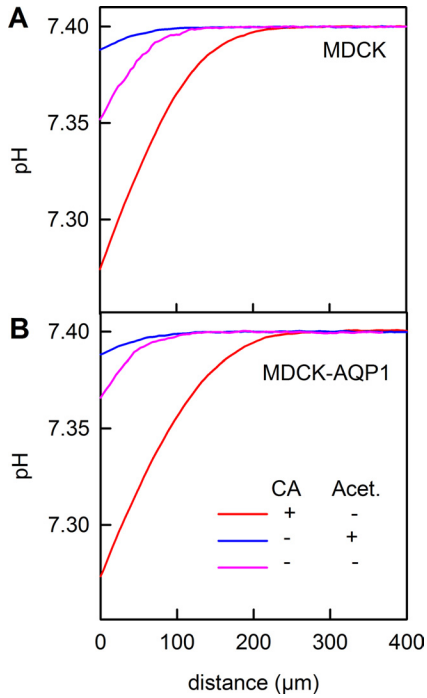

FIGURE 7. **CA activity but not aquaporins regulate P_{CO2}.** pH profiles measured in the presence of a 1 mM CO_2 gradient (Π_{CO2} = 33.3 mm Hg; 20 mM HCO_3^-) across monolayers from MDCK (*A*) and MDCK-AQP1 cells (*B*). CO_2 fluxes through AQP1 expressing and non-expressing cells were identical ($n > 9$). The *red* profiles were measured in the presence of 2 mg/ml CA in the bathing medium, the *pink* profiles were measured without external CA, and the *blue* profiles were measured with 1 mM acetazolamide (*Acet.*) to inhibit the intracellular CA. The bulk solution consisted of Hanks' Buffered Salt Solution with 20 mM HEPES in addition (pH = 7.4, 37 °C).

(a 14-fold drop) indicates that the system may be reaction-limited (Fig. 8) rather than membrane-limited.

The implication of this result is that CA is perfectly suited to regulate CO_2 transport. This result contrasts with a large body of literature (for an overview, see Ref. 16), which ascribes a role for the regulation of CO_2 permeability to aquaporins. To test whether aquaporins may reverse the inhibitory effect of missing CA activity

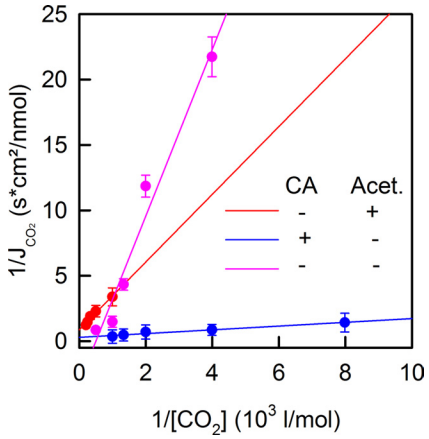

FIGURE 8. **Determining P_{CO2}.** The slope of $1/J_{CO2} = f(1/[CO_2])$ is inversely proportional to P_{CO2} (compare Equation 2). The urinary mouse bladder ($P_{CO2} \sim 1.6 \times 10^{-4}$ cm/s) is 45× less permeable than MDCK cells with external CA (7×10^{-3} cm/s) and three times less permeable than MDCK monolayer with blocked intracellular CA (5.1×10^{-4} cm/s). We conclude that CA regulates membrane P_{CO2}. *Acet.*, acetazolamide.

on CO_2 transport, we repeated the experiments in aquaporin-1-overexpressing cells (11). The measured pH profiles in presence and absence of AQP1 (Fig. 7) show no difference. These results suggest that AQP1 does not facilitate CO_2 transport and that the flux is just limited by CO_2 hydration/dehydration kinetics. Furthermore, these results also confirm our earlier studies showing that AQP1 does not transport CO_2 (11).

DISCUSSION

When the kidney generates acidic urine, partial CO_2 pressure Π_{CO2} of urine reaches 80–100 mm Hg, 3–4-fold higher than blood Π_{CO2} (8) (9, 10). This indicates that CO_2 equilibrates across the bladder very slowly and suggests that the bladder is a barrier to CO_2 transport. Such a conclusion contrasts with our earlier observation that CO_2 transport across membranes is not limited by the membrane itself but by adjacent USLs (11). P_{CO2} of lipid membranes is so high that it exceeds the permeabilities to ammonia or water by at least 2 orders of magnitude (17). In contrast, the bladder shows a ~45-fold reduced P_{CO2} compared with monolayer of MDCK cells. Such an unusual low P_{CO2} across the bladder could be due to: (*a*) the uroplakin plaques that cover the urothelium, (*b*) a large unstirred layer created by the four to five layers of cells, or (*c*) slow kinetics of CO_2 hydration and/or dehydration.

Our results show that, in contrast to water and solute flux, removal of uroplakins by protamine sulfate treatment or by genetic ablation does not influence the flux of CO_2. A USL created by the four to five cell layers of the urothelium would be ~50 μm in size. A simple calculation shows that its permeability $P_{USL} = D_{CO2}/\delta = 2.9 \times 10^{-5}/5 \times 10^{-3}$ cm/s $= 6 \times 10^{-3}$ cm/s is much too large to explain the ~45-fold decrease in P_{CO2} of the bladder compared with a monolayer of MDCK cells.

Such a large reduction must be due to slow CO_2 hydration-dehydration kinetics caused by lack of CA in the urothelium. Inhibition of the CA in MDCK cells decreased apparent P_{CO2} by a factor of 10 and thus recapitulated the reaction limited transport of the bladder, validating our conclusion. A series connection of four or five monolayers, as represented by the bladder epithelium, would have a 40–50-fold lower apparent P_{CO2} because CO_2 must undergo the same chemical reaction every time it crosses a membrane on its way. These observations suggest that CA activity can regulate P_{CO2}.

Sometimes regulation of P_{CO2} is attributed to aquaporins. But even if aquaporin-1 could facilitate CO_2 transport in red blood cells and in *Xenopus* oocytes (11, 18–20), it would still transport only the neutral species. This means that CO_2 transport must be limited in the absence of CA, even if AQP1 is expressed because there is simply no CO_2 available for transport. These considerations are in perfect agreement with our experiment (Fig. 7). That is, the identification of membrane barriers to CO_2 transport does not necessarily imply that proteinaceous transport machineries are required. It may simply mean that CA activity is low as we have now shown for the bladder epithelium.

With a partition coefficient of 1.3 (hexadecane), CO_2 partitions into lipids as easily as it does into an aqueous pore. Thus, the inability of AQPs to facilitate CO_2 transport is already implied by the comparison of the total membrane surface area A of 3.2×10^{-13} cm^2 of the aquaporin tetramer, and the maximal pore area of 3×10^{-15} cm^2 provided by the tetramer for CO_2 diffusion. A more quantitative analysis must also account for mobility differences in the two environments. Thus, the ratio J_{Lip}/J_{AQP} of the fluxes through a lipid patch the size of an aquaporin tetramer and through four aqueous pores is calculated as follows,

$$\frac{J_L}{J_{AQP}} = \frac{P_M A[CO_2]}{4p[CO_2]} = \frac{3.2\ \text{cm/s} \times 3.2 \times 10^{-13}\ \text{cm}^2}{4 \times 1.2 \times 10^{-14}\ \text{cm}^3\text{/s}} = 21 \quad \text{(Eq. 4)}$$

where P_M and p are the lower limit of membrane permeability to CO_2 (11) and the upper limit of single channel CO_2 permeability, respectively. The factor four in the denominator indicates the four pores of the tetramer. Given that CO_2 is highly diluted in the aqueous solution (*i.e.* that the ratio of H_2O to CO_2 concentrations is roughly equal to 10^5), it is safe to assume that there is no more than one CO_2 molecule in the pore at one time. Because molecules cannot pass each other in single file transport, this leads to $p = p_f/10$, where 10 indicates the total number of molecules in the pore and $p_f = 11.7 \times 10^{-14}$ cm^3/s (32) denotes single pore permeability to H_2O. This calculation does not account for the central pore. Molecular dynamics simulations, however, predict that the central pore is either entirely non-conductive (33) or its permeability to CO_2 is smaller than p_f (34). We conclude that $J_{Lip}/J_{AQP} > 1$, indicating that aquaporin insertion into a membrane tends to lower its permeability. This result is in agreement with previous MD simulations of CO_2 passages through lipid membranes and aquaporins (21, 34). Ammonia is the only gas, which according to the solubility diffusion model, may be facilitated by presence of channel such as an aquaporin (22).

We have shown that expression of aquaporin-1 in MDCK cells leads to a 3-fold increase in water permeability (11) but with no detectable change in CO_2 permeability, which is consistent with our earlier results (11). Presence or absence of aquaporin-1 in cells lacking CA activity did not alter the CO_2

flux. The urothelium functions as a low permeability barrier to CO_2 due to lack of detectable CA in the urothelium. We suggest that P_{CO2} of biological barriers is generally regulated by CA activity.

REFERENCES

1. Chang, A., Hammond, T. G., Sun, T. T., and Zeidel, M. L. (1994) Permeability properties of the mammalian bladder apical membrane. *Am. J. Physiol. Cell Physiol.* **267,** C1483–C1492
2. Zeidel, M. L. (1996) Low permeabilities of apical membranes of barrier epithelia: What makes watertight membranes watertight? *Am. J. Physiol.* **271,** F243–F245
3. Hu, P., Meyers, S., Liang, F. X., Deng, F. M., Kachar, B., Zeidel, M. L., and Sun, T.T. (2002) Role of membrane proteins in permeability barrier function: Uroplakin ablation elevates urothelial permeability. *Am. J. Physiol. Renal Physiol.* **283,** F1200–F1207
4. Lavelle, J., Meyers, S., Ramage, R., Bastacky, S., Doty, D., Apodaca, G., and Zeidel, M. L. (2002) Bladder permeability barrier: Recovery from selective injury of surface epithelial cells. *Am. J. Physiol. Renal Physiol.* **283,** F242–253
5. Kachar, B., Liang, F., Lins, U., Ding, M., Wu, X. R., Stoffler, D., Aebi, U., and Sun, T. T. (1999) Three-dimensional analysis of the 16 nm urothelial plaque particle: Luminal surface exposure, preferential head-to-head interaction, and hinge formation. *J. Mol. Biol.* **285,** 595–608
6. Khandelwal, P., Abraham, S. N., and Apodaca, G. (2009) Cell biology and physiology of the uroepithelium. *Am. J. Physiol. Renal Physiol.* **297,** F1477–1501
7. Lavelle, J., Meyers, S., Ramage, R., Doty, D., Bastacky, S., Apodaca, G., and Zeidel, M. (2001) Protamine sulfate-induced cystitis: A model of selective cytodestruction of the urothelium. *Urology* **57,** 113
8. Weinstein, A. M. (1998) A mathematical model of the inner medullary collecting duct of the rat: Pathways for Na and K transport. *Am. J. Physiol.* **274,** F841–F855
9. DuBose, T. D., Jr. (1982) Hydrogen ion secretion by the collecting duct as a determinant of the urine to blood PCO2 gradient in alkaline urine. *J. Clin. Invest.* **69,** 145–156
10. Ryberg, C. (1948) Some investigations on the carbon dioxide tension of the urine in man. *Acta Physiol. Scand.* **15,** 123–139
11. Missner, A., Kügler, P., Saparov, S. M., Sommer, K., Mathai, J. C., Zeidel, M. L., and Pohl, P. (2008) Carbon dioxide transport through membranes. *J. Biol. Chem.* **283,** 25340–25347
12. Mathai, J. C., Missner, A., Kügler, P., Saparov, S. M., Zeidel, M. L., Lee, J. K., and Pohl, P. (2009) No facilitator required for membrane transport of hydrogen sulfide. *Proc. Natl. Acad. Sci. U.S.A.* **106,** 16633–16638
13. Negrete, H. O., Lavelle, J. P., Berg, J., Lewis, S. A., and Zeidel, M. L. (1996) Permeability properties of the intact mammalian bladder epithelium. *Am. J. Physiol.* **271,** F886–F894
14. Aboushwareb, T., Zhou, G., Deng, F. M., Turner, C., Andersson, K. E., Tar, M., Zhao, W., Melman, A., D'Agostino, R. Jr., Sun, T. T., and Christ, G. J. (2009) Alterations in bladder function associated with urothelial defects in uroplakin II and IIIa knock-out mice. *Neurourol. Urodyn.* **28,** 1028–1033
15. Gutknecht, J., Bisson, M. A., and Tosteson, F. C. (1977) Diffusion of carbon dioxide through lipid bilayer membranes: Effects of carbonic anhydrase, bicarbonate, and unstirred layers. *J. Gen. Physiol.* **69,** 779–794
16. Boron, W. F., Endeward, V., Gros, G., Musa-Aziz, R., and Pohl, P. (2011) Intrinsic CO_2 permeability of cell membranes and potential biological relevance of CO_2 channels. *ChemPhysChem* **12,** 1017–1019
17. Saparov, S. M., Liu, K., Agre, P., and Pohl, P. (2007) Fast and selective ammonia transport by aquaporin-8. *J. Biol. Chem.* **282,** 5296–5301
18. Endeward, V., Musa-Aziz, R., Cooper, G. J., Chen, L. M., Pelletier, M. F., Virkki, L. V., Supuran, C. T., King, L. S., Boron, W. F., and Gros, G. (2006) Evidence that aquaporin 1 is a major pathway for CO_2 transport across the human erythrocyte membrane. *FASEB J.* **20,** 1974–1981
19. Fang, X., Yang, B., Matthay, M. A., and Verkman, A. S. (2002) Evidence against aquaporin-1-dependent CO2 permeability in lung and kidney. *J. Physiol.* **542,** 63–69
20. Musa-Aziz, R., Chen, L. M., Pelletier, M. F., and Boron, W. F. (2009) Relative CO2/NH3 selectivities of AQP1, AQP4, AQP5, AmtB, and RhAG. *Proc. Natl. Acad. Sci. U.S.A.* **106,** 5406–5411
21. Hub, J. S., and de Groot, B. L. (2008) Mechanism of selectivity in aquaporins and aquaglyceroporins. *Proc. Natl. Acad. Sci. U.S.A.* **105,** 1198–1203
22. Missner, A., and Pohl, P. (2009) 110 years of the Meyer-Overton rule: predicting membrane permeability of gases and other small compounds. *ChemPhysChem* **10,** 1405–1414
23. Hu, P., Deng, F. M., Liang, F. X., Hu, C. M., Auerbach, A. B., Shapiro, E., Wu, X. R., Kachar, B., and Sun, T. T. (2000) Ablation of uroplakin III gene results in small urothelial plaques, urothelial leakage, and vesicoureteral reflux. *J. Cell. Biol.* **151,** 961–972
24. Kong, X. T., Deng, F. M., Hu, P., Liang, F. X., Zhou, G., Auerbach, A. B., Genieser, N., Nelson, P. K., Robbins, E. S., Shapiro, E., Kachar, B., and Sun, T. T. (2004) Roles of uroplakins in plaque formation, umbrella cell enlargement, and urinary tract diseases. *J. Cell. Biol.* **167,** 1195–1204
25. Hodges, S. J., Zhou, G., Deng, F. M., Aboushwareb, T., Turner, C., Andersson, K. E., Santago, P., Case, D., Sun, T. T., and Christ, G. J. (2008) Voiding pattern analysis as a surrogate for cystometric evaluation in uroplakin II knock-out mice. *J. Urol.* **179,** 2046–2051
26. Deng, F. M., Liang, F. X., Tu, L., Resing, K. A., Hu, P., Supino, M., Hu, C. C., Zhou, G., Ding, M., Kreibich, G., and Sun, T. T. (2002) Uroplakin IIIb, a urothelial differentiation marker, dimerizes with uroplakin Ib as an early step of urothelial plaque assembly. *J. Cell. Biol.* **159,** 685–694
27. Lavelle, J. P., Apodaca, G., Meyers, S. A., Ruiz, W. G., and Zeidel, M. L. (1998) Disruption of guinea pig urinary bladder permeability barrier in noninfectious cystitis. *Am. J. Physiol.* **274,** F205–F214
28. Wilbur, K. M., and Anderson, N. G. (1948) Electrometric and colorimetric determination of carbonic anhydrase. *J. Biol. Chem.* **176,** 147–154
29. Hill, W. G., Meyers, S., von Bodungen, M., Apodaca, G., Dedman, J. R., Kaetzel, M. A., and Zeidel, M. L. (2008) Studies on localization and function of annexin A4a within urinary bladder epithelium using a mouse knock-out model. *Am. J. Physiol. Renal Physiol.* **294,** F919–927
30. Deen, P. M., Nielsen, S., Bindels, R. J., and van Os, C. H. (1997) Apical and basolateral expression of aquaporin-1 in transfected MDCK and LLC-PK cells and functional evaluation of their transcellular osmotic water permeabilities. *Pflugers Arch.* **433,** 780–787
31. Pohl, P., Rosenfeld, E., and Millner, R. (1993) Effects of ultrasound on the steady-state transmembrane pH gradient and the permeability of acetic acid through bilayer lipid membranes. *Biochim. Biophys. Acta* **1145,** 279–283
32. Zeidel, M. L., Ambudkar, S. V., Smith, B. L., and Agre, P. (1992) Reconstitution of functional water channels in liposomes containing purified red cell CHIP28 protein. *Biochemistry* **31,** 7436–7440
33. Hub, J. S., and de Groot, B. L. (2006) Does CO_2 permeate through aquaporin-1? *Biophys. J.* **91,** 842–848
34. Wang, Y., Cohen, J., Boron, W. F., Schulten, K., and Tajkhorshid, E. (2007) Exploring gas permeability of cellular membranes and membrane channels with molecular dynamics. *J. Struct. Biol.* **157,** 534–544